Supplemental material to "Aerothermodynamics of a sphere in a monatomic gas based on *ab initio* interatomic potentials over a wide range of gas rarefaction: subsonic flows"

Felix Sharipov [1]† and Alexey N. Volkov [2]

[1]Departamento de Física, Universidade Federal do Paraná, Caixa Postal 19044, Curitiba 81531-980, Brazil
[2]Department of Mechanical Engineering, University of Alabama, 7th Avenue, Tuscaloosa, AL 35487, USA

1. Sphere drag and heat transfer coefficients in the free-molecular flow regime

The drag C_D^* and average heat transfer C_Q^* coefficients of a sphere in the free molecular-flow regime calculated with Eqs. (3.1) and (3.2) as functions of TMAC α_t and NEAC α_n at $Ma = 0.2$ are shown in Figure 1. These results indicate that the variation of α_n results in the qualitatively different variations of C_D^* and C_Q^* at $T_w/T_\infty = 1$ and $T_w/T_\infty > 1$. In a nearly isothermal flow at $T_w/T_\infty = 1$, C_D^* decreases and C_Q^* increases with increasing α_n. At $T_w/T_\infty = 10/3$, these trends are reverse. The dependencies of C_D^* and C_Q^* on α_t and α_n shown in Figure 1 are characteristic for free-molecular subsonic flows over a sphere at various Ma.

2. Analysis of numerical errors

The coefficients C_D^* and C_Q^* for hard sphere molecular model calculated using several combinations of the parameters Δx, Δt, and R_d are given in Tables 1, 2, and 3 for $\delta = 0.1$, 1, and 10, respectively. These data show the convergence of C_D^* within 0.5% and C_Q^* within 1% when the parameters Δx and Δt decrease and the parameter R_d increases.

To estimate the statistical scattering of C_D^* and C_Q^*, their mean values are calculated as

$$\bar{C} = \frac{1}{N_s}\sum_{i=1}^{N_s} C_i, \tag{2.1}$$

† Email address for correspondence: sharipov@fisica.ufpr.br

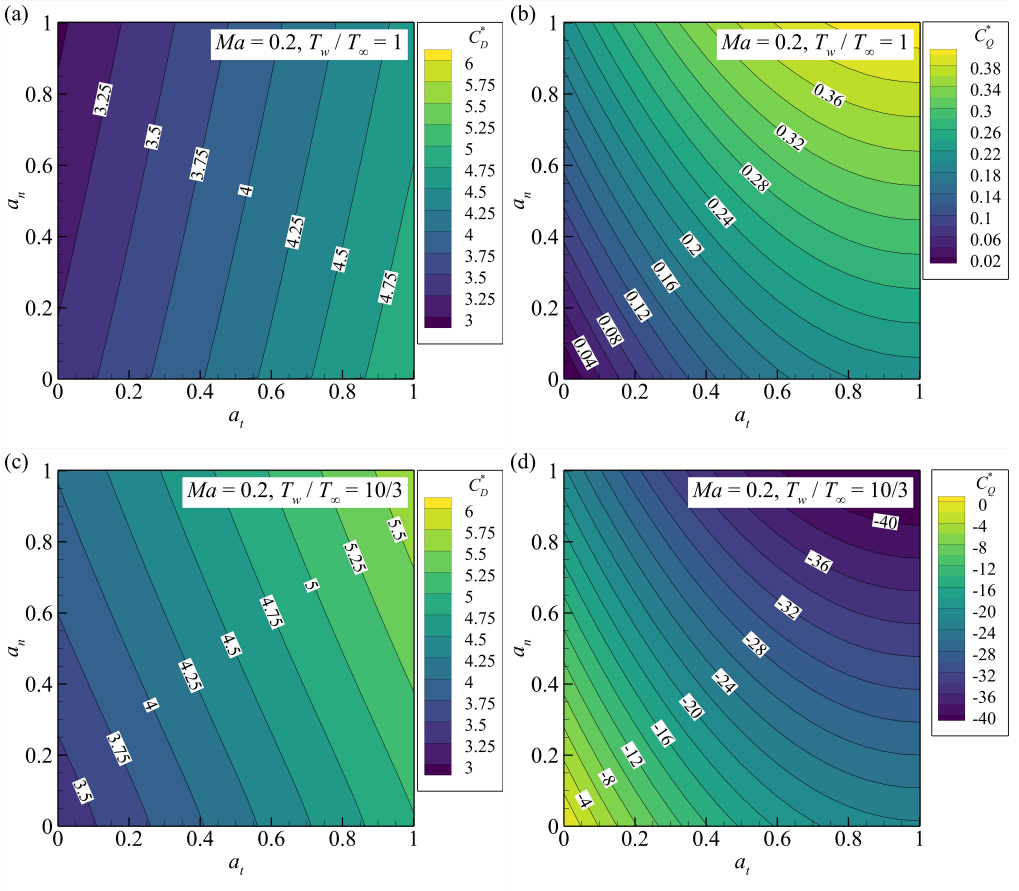

Figure 1: Drag C_D^* (a,c) and average heat transfer C_Q^* (b,d) coefficients of a sphere in the free molecular-flow regime calculated with Eqs. (3.1) and (3.2) as functions of TMAC α_t and NEAC α_n at $Ma = 0.2$ for $T_w/T_\infty = 1$ (a,b) and $10/3$ (c,d).

where $N_s \gg 1$ is the number of the time steps and C_i is C_D^* or C_Q^* calculated in one time step. The relative standard error of the mean is given as

$$\sigma = \frac{1}{\bar{C} N_s} \sqrt{\sum_{i=1}^{N_s} \left(C_i - \bar{C}\right)^2} \times 100\%. \tag{2.2}$$

The calculations lasted until the values of σ became smaller than 0.1%.

3. Tables with calculated values of the drag and average energy transfer coefficients

Table 4 contains the values of the drag C_D^* and average energy transfer C_Q^{**} coefficients as well as Stanton number St and adiabatic surface temperature T_{ad}/T_∞ obtained in the DSMC simulations for helium based on the model of diffuse scattering.

$\frac{R}{\Delta x}$	$\Delta t \frac{v_\infty}{R}$	$\frac{R_d}{R}$	$Ma = 0.1$ C_D^*	$Ma = 0.2$ C_D^*	C_Q^*	$Ma = 0.5$ C_D^*	C_Q^*
40	0.005	4	4.476	4.495	0.3991	4.586	0.4116
20	0.002	4	4.475	4.493	0.3928	4.595	0.4137
20	0.005	4	4.477	4.497	0.3997	4.595	0.4133
20	0.005	8	4.466	4.476	0.4080	4.560	0.4070
20	0.005	12	4.440	4.474	0.4021	4.557	0.4078

Table 1: Convergence of drag C_D^* and energy transfer C_Q^* coefficients with respect to domain size R_d, cell size Δx, and time step Δt at $\delta = 0.1$.

$\frac{R}{\Delta x}$	$\Delta t \frac{v_\infty}{R}$	$\frac{R_d}{R}$	$Ma = 0.1$ C_D^*	$Ma = 0.2$ C_D^*	C_Q^*	$Ma = 0.5$ C_D^*	C_Q^*
40	0.005	4	3.524	3.527	0.2779	3.570	0.2831
20	0.002	4	3.519	3.523	0.2790	3.574	0.2839
20	0.005	4	3.510	3.525	0.2763	3.572	0.2841
20	0.005	8	3.329	3.350	0.2614	3.454	0.2692
20	0.005	16	3.221	3.263	0.2511	3.412	0.2648
20	0.005	20	3.207	3.247	0.2522	3.413	0.2646

Table 2: Convergence of drag C_D^* and energy transfer C_Q^* coefficients with respect to domain size R_d, cell size Δx, and time step Δt at $\delta = 1$.

$\Delta t \frac{v_\infty}{R}$	$\frac{R_d}{R}$	$Ma = 0.1$ $\frac{R}{\Delta x}$	C_D^*	$Ma = 0.2$ $\frac{R}{\Delta x}$	C_D^*	C_Q^*	$Ma = 0.5$ C_D^*	C_Q^*
0.002	4	60	1.047	100	1.132	0.07472	1.411	0.08740
0.001	4	40	1.049	60	1.135	0.07459	1.413	0.08755
0.002	4	40	1.052	60	1.134	0.07425	1.413	0.08748
0.002	12	40	0.8425	60	0.9744	0.06731	1.296	0.08399
0.002	20	40	0.8291	60	0.9621	0.06972	1.287	0.08413
0.002	30	40	0.8169	60	0.9581	0.06955	1.287	0.08423
0.002	40	40	0.8115					

Table 3: Convergence of drag C_D^* and energy transfer C_Q^* coefficients with respect to domain size R_d, cell size Δx, and time step Δt at $\delta = 10$.

4. Comparison of the calculated values of the adiabatic surface temperature with a semi-empirical equation

Koshmarov & Svirshevskii (1993) proposed the following equation for the adiabatic surface temperature of a sphere in a monatomic gas

$$\frac{T_{ad}}{T_\infty} = 1 + \frac{2}{5} S^2 \zeta, \tag{4.1}$$

Ma	δ	T_w(K)	C_D^*	C_Q^{**}	St	T_{ad}/T_∞
0.1	0.1	100	3.90	0.494	2.450	1.005
		600	4.95	-0.732	2.453	
		1000	5.45	-1.71	2.455	
	1	100	2.91	0.508	2.176	1.004
		600	3.43	-0.724	2.109	
		1000	3.74	-1.72	2.081	
	10	100	0.676	0.617	0.788	1.003
		600	0.934	-0.674	0.906	
		1000	0.998	-1.71	0.929	
0.2	0.1	100	3.94	0.438	1.234	1.021
		600	4.98	-0.63	1.235	
		1000	5.49	-1.45	1.236	
	1	100	2.97	0.448	1.096	1.016
		600	3.52	-0.628	1.064	
		1000	3.83	-1.44	1.051	
	10	100	0.830	0.514	0.458	1.010
		600	1.05	-0.579	0.494	
		1000	1.13	-1.42	0.497	
0.5	0.1	100	4.03	0.158	0.515	1.132
		600	5.07	-0.271	0.517	
		1000	5.6	-0.649	0.518	
	1	100	3.15	0.186	0.444	1.104
		600	3.69	-0.294	0.431	
		1000	3.98	-0.692	0.426	
	10	100	1.17	0.248	0.226	1.063
		600	1.37	-0.316	0.224	
		1000	1.44	-0.746	0.219	

Table 4: Drag C_D^* and average energy transfer C_Q^{**} coefficients, Stanton number St, and adiabatic surface temperature T_{ad}/T_∞ vs. Mach numebr Ma, rarefaction parameter δ, and surface temperature T_w.

where $\zeta = (T_{ad} - T_\infty)/(T_0 - T_\infty)$ is the recovery factor given by the equation

$$\zeta = \zeta_c + (\zeta_m - \zeta_c)\left\{1 + 4.5\left[\frac{2}{Z} - 1\right]^2\right\}^{-1}. \tag{4.2}$$

In Eq. (4.2), $\zeta_c = 0.908$ is the recovery factor in the continuum flow regime and

$$\zeta_m = \frac{5}{4S^2}\left[\left(S^2 + \frac{1}{2}\right) - \frac{\sqrt{\pi}\,\mathrm{erf}(S)}{\sqrt{\pi}\left(2S^2+1\right)\,\mathrm{erf}(S) + 2S\exp(-S^2)}\right]. \tag{4.3}$$

is the recovery factor in the free-molecular flow regime at diffuse scattering, where $S = \sqrt{5/6}Ma$ and Ma is the Mach number. The variable Z in Eq. (4.2) describes the transition from free molecular to continuum flow and is defined as

$$Z = \frac{2Nu_c}{Nu_m + Nu_c}, \tag{4.4}$$

where

$$Nu_c = 2 + 0.03 Pr^{0.33} Re^{0.54} + 0.35 Pr^{0.356} Re^{0.58} \tag{4.5}$$

is the Nusselt number in the continuum flow regime and

$$Nu_m = \frac{PrRe}{5\sqrt{\pi}S^2}\left[\sqrt{\pi}\left(S^2 + \frac{1}{2}\right)\,\mathrm{erf}(S) + S\exp(-S^2)\right] \tag{4.6}$$

is the Nusselt number in the free molecular flow regime at diffuse scattering. In Eq. (4.5) and (4.6), Pr and Re are the Prandtl and Reynolds numbers. Equation (4.6) transformed to the Stanton number $St = Nu/(Pr\ Re)$ coincides with Eq. (5.2) from the main text of the paper.

The comparison between the adiabatic temperature calculated based on Eq. (4.1)- (4.6) and obtained in the DSMC simulations in the present work is given in Figure 2. These results indicate that the equation proposed by Koshmarov & Svirshevskii (1993) overestimates the values of T_{ad}/T_∞ found in DSMC simulations in the whole range of δ and Ma considered in simulations. This discrepancy can be attributed to two factors. First, at relatively large Re, the discrepancy appears because the value of the recovery factor $r_c = 0.908$ adopted by Koshmarov & Svirshevskii (1993) for the continuum flow regime is a good approximation only at relatively small Ma, as can be concluded from the comparison of results shown for $Ma = 0.1$ in Figure 2(a). Second, the semi-empirical equation systematically predicts faster increase in the recovery factor compared to the results of DSMC simulations in the transitional flow regime with decreasing Re or δ.

5. Comparison of the calculated values of the Stanton number with semi-empirical equations

Kavanau (1955) suggested a semi-empirical equation for the Nusselt number Nu of a sphere in the transitional flow regime in the form

$$Nu = \frac{Nu_c}{1 + 3.42\dfrac{Ma}{Pr\ Re}Nu_c}, \tag{5.1}$$

where $Nu_c = Nu_c(Re, Pr)$ is the value of the sphere Nusselt number in the continuum flow regime. The latter can be calculated, as suggested, e.g., by Nelson & Fields (1996), with the equation (Eckert & Drake (1959))

$$Nu_c = 2 + 0.459\ Pr^{0.33}\ Re^{0.55}. \tag{5.2}$$

Eq. (5.1) is designed to fit the experimental data on the sphere heat transfer at $0.1 \leqslant Ma \leqslant 0.69$ and $1.75 \leqslant Re \leqslant 124$.

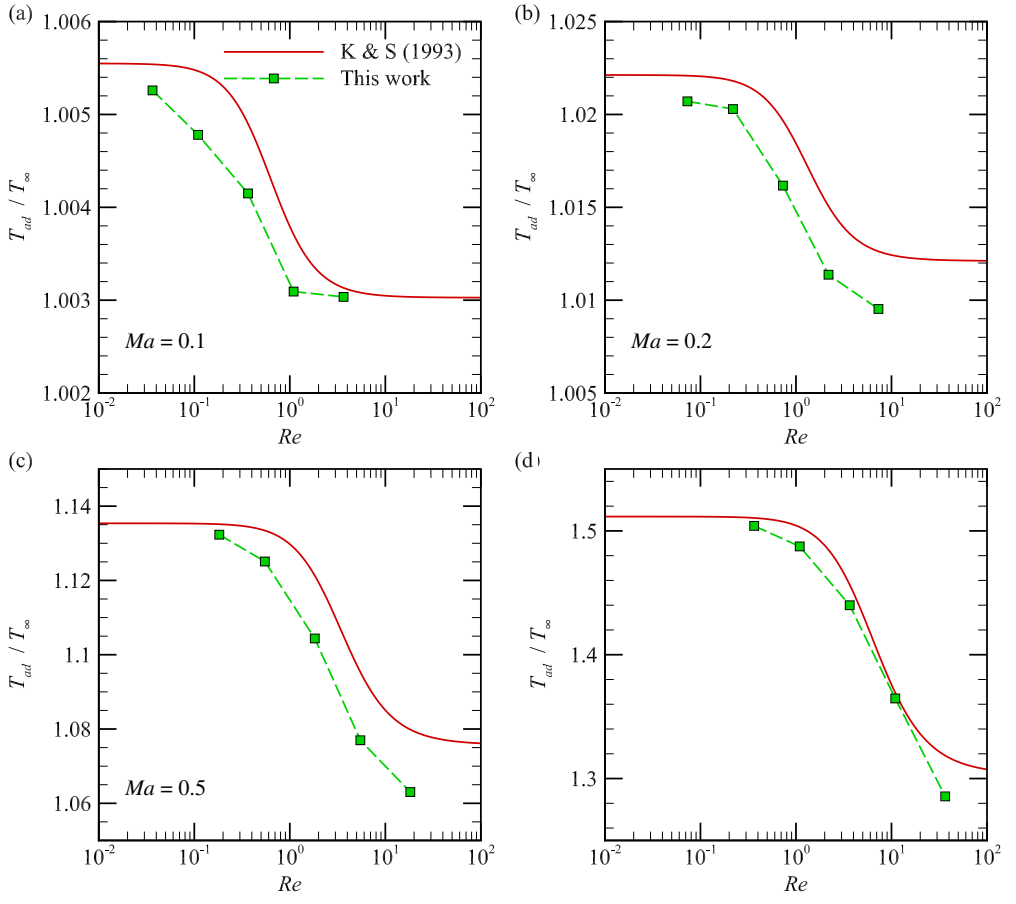

Figure 2: Adiabatic surface temperature T_{ad}/T_∞ of the sphere versus Reynolds number Re predicted by the semi-empirical equations (4.1)–(4.6) by Koshmarov & Svirshevskii (1993) (K & S, solid curves) and obtained in the DSMC simulations in the present work (symbols and dashed curves) at Ma = 0.1 (a), 0.2 (b), 0.5 (c), and 1 (d)). The DSMC simulations are performed for helium and diffuse scattering model at T_∞ = 300 K. All calculations are performed assuming that Pr = 0.67.

Koshmarov & Svirshevskii (1993) proposed another equation for the sphere Nusselt number in all flow regimes in the form

$$Nu = (Nu_m + Nu_c)\bar{N} - Nu_c, \tag{5.3}$$

where

$$\bar{N} = Z\left[1 + \left(\frac{Z}{2}\right)^{3/2}\right]^{-1}, \tag{5.4}$$

the value of Z is calculated based on Eq. (4.4), and the sphere Nusselt numbers in the continuum, Nu_c, and free-molecular, Nu_m, flow regimes are given by Eq. (4.5) and (4.6),

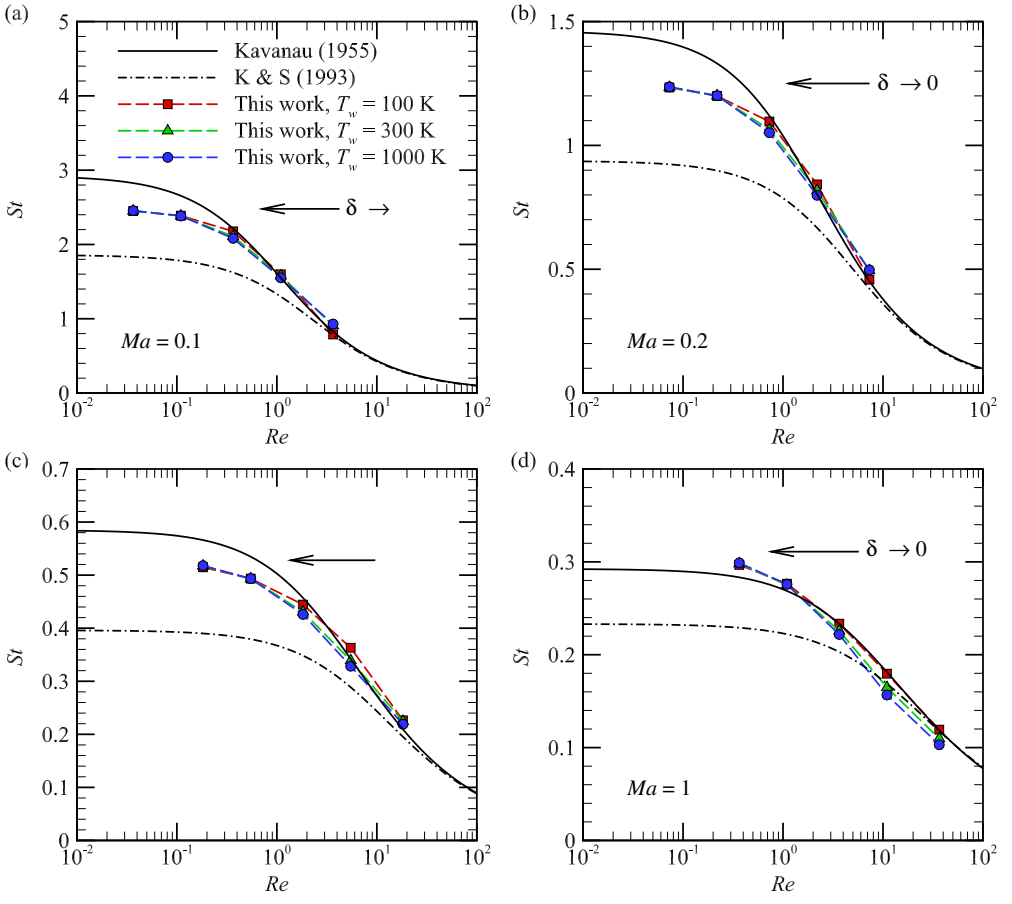

Figure 3: Stanton number St versus Reynolds number Re predicted by the semi-empirical equation (5.1) by Kavanau (1955) (solid curves), semi-empirical equation (5.3) by Koshmarov & Svirshevskii (1993) (K & S, dash-dotted curves) and obtained in the DSMC simulations in the present work (symbols and dashed curves) at Ma = 0.1 (a), 0.2 (b), 0.5 (c), and 1 (d). The equation by Kavanau (1955) is used together with Eq. (5.2) for the continuum flow regime. The DSMC simulations are performed for helium and diffuse scattering model at T_∞ = 300 K. All calculations are performed assuming that Pr = 0.67. The horizontal arrows mark the values of St in the free-molecular flow regime calculated with Eq. (4.6).

respectively. Eq. (5.3) is derived to fit the experimental data on the sphere heat transfer at $0.1 \leqslant Ma \leqslant 9.7$ and $0.6 \leqslant T_w/T_\infty \leqslant 1.06$.

The comparison of the values of the Stanton number St obtained in the DSMC simulations in the present work with the dependencies of $St = Nu/(Pr\ Re)$ calculated based on semi-empirical Eq. (5.1) and (5.3) is presented in Figure 3. The semi-empirical equation by Kavanau (1955) agrees well with the DSMC data points in the range of $Re \geqslant 1$ in the whole range of the Mach number considered. At smaller Re, this equation overestimates the Stanton number at $Ma = 0.1 - -0.5$ and underestimates St at $Ma = 1$ since this equation

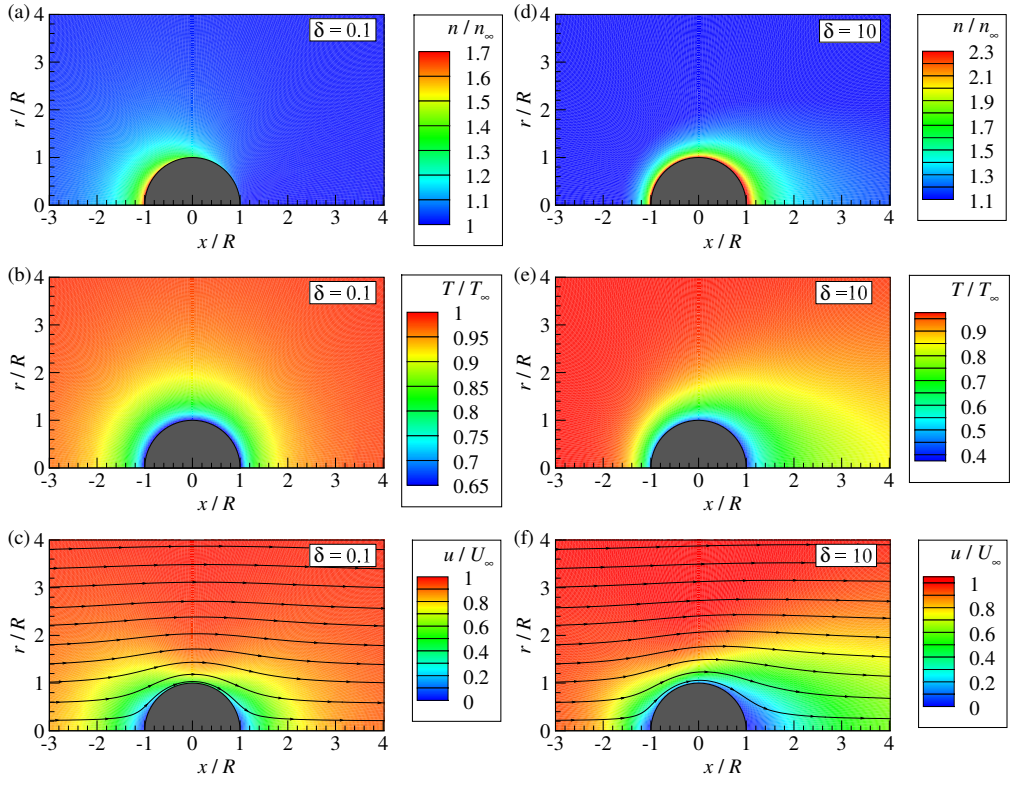

Figure 4: Fields of density n/n_∞ (a,d), temperature T/T_∞ (b,e), and flow speed u/U_∞ with streamlines (c,f) of helium at $Ma = 0.2$, diffuse scattering, $T_\infty = 300$ K, and $T_w = 100$ K: (a), (b), (c) - $\delta = 0.1$, (d), (e), (f) - $\delta = 10$.

cannot predict thr correct asymptotic behavior of St in the free-molecular flow regime when $Re \to 0$ at $Ma = const$. On the contrary, the semi-empirical equation by Koshmarov & Svirshevskii (1993) tends to underestimate the sphere Stanton number in the whole range of Re corresponding to the transitional flow regimes and, moreover, does not demonstrate the expected correct asymptotic behaviour in the limit of free-molecular flow described by Eq. (4.6). The reason for this deficiency of Eq. (5.3) is not clear.

6. Flow fields around a cold sphere at $T_w = 100$ K

The fields of gas density, temperature, and speed in the flow over a cold sphere with a surface temperature of $T_w = 100$ K at $Ma = 0.2$ are shown in Figure 4. These fields can be compared with the corresponding fields for a thermally neutral ($T_w = 300$ K) and hot ($T_w = 1000$ K) spheres shown in Figures 8 and 10 of the main paper, respectively. This comparison indicates that at $\delta = 0.1$ in the flow over a cold sphere, the region of the increased gas density appears primarily in front of the sphere, while in the flow over a hot sphere the region of reduced

density appears behind the sphere. At $\delta = 10$, the region of disturbed flow tends to reduce its size upstream the sphere and be more elongated along the flow direction behind the sphere.

REFERENCES

Eckert, E R T & Drake, R W 1959 *Heat and Mass Transfer*, 2nd edn. New York: McGraw-Hill.

Kavanau, L L 1955 Heat transfer from spheres to a rarefied gas in subsonic flow. *Trans. ASME* **77**, 617–623.

Koshmarov, Y A & Svirshevskii, S B 1993 *Aero- and Hydromechanics*. Moscow: Mashinostroenie, [in Russian].

Nelson, H F & Fields, J C 1996 Heat transfer in two-phase solid-rocket plumes. *J. Spacecraft and Rockets* **33**, 494–500.